Microstructure and nonlinear electrical characteristics of SnO_2·CuO·Nb_2O_5 system

CHUN-MING WANG*, JIN-FENG WANG, WEN-BIN SU, GUO-ZHONG ZANG, PENG QI
School of Physics and Microelectronics, Shandong University, Jinan 250100, People's Republic of China
E-mail: sdwangcm@mail.edu.cn, sdwangcm@mail.sdu.edu.cn

Published online: 1 November 2005

In recent decades tin oxide based ceramics have been studied and developed for numerous fields of application such as electronics, electro techniques, electrochemistry, catalysis, biotechnology, nuclear technology, chemical technologies, metallurgy [1]. As ceramic varistor materials, tin oxide has been extensively studied experimentally and theoretically recently, since this oxide shows excellent nonlinearity when doped with minor other oxides, such as CoO, ZnO, Ni_2O_3, Ta_2O_5, Nb_2O_5 and rare-earth oxides [2–7]. Recently, nonlinear electrical properties were obtained for a basic ceramic system based on SnO_2·CuO·Ta_2O_5 ternary varistor ceramics [8, 9].

In this letter, compared with the CuO and Ta_2O_5-doped SnO_2 system, the electrical properties (electric field as a function of current density behavior) of CuO and Nb_2O_5-doped SnO_2 system as well as the microstructure development are described. We obtained some satisfying results that the nonlinear coefficient reaches 34.4 and the relative density of the sample is up to 94% of the theoretical density.

Tin oxide varistors were produced by the conventional ceramic fabrication procedure reported earlier [6, 8]. The materials used in the present study were analytical grades of SnO_2 (99.5% purity), CuO (98.0%), Nb_2O_5 (99.5%) and Ta_2O_5 (99.5%) to the composition of 99.00 mol% SnO_2 + 1.00 mol% CuO (named SC), 98.95 mol% SnO_2 + 1.00 mol% CuO + 0.05 mol% Nb_2O_5 (SCNb) and 98.95 mol% SnO_2 + 1.00 mol% CuO + 0.05 mol% Ta_2O_5 (SCTa). The samples were sintered at 1400 °C for 1 hr and cooled to room temperature freely. The ceramic phases analysis was conducted by X-ray diffraction (XRD, XD-3, PGeneral) patterns. The density (ρ) and the theoretical density (ρ_{rt}) were obtained by the Archimedes method and related to the theoretical density of SnO_2 (=6.95 g cm^{-3}). Microstructure characterization of the sintered ceramics was conducted by scanning electron microscopy (SEM, JXA-840, JEOL). The grain sizes (d) were calculated by microstructure linear analysis. For the direct-current density—electrical field (J–E) characterization, silver electrodes (1 cm^2) were made on both surfaces of the sintered discs and fired for 20 min at 550 °C in air. A 2410 High-Voltage SourceMeter (Keithley) was used for J–E measurement.

The surface XRD patterns of selected samples are shown in Fig. 1. The JCPDS cards (SnO_2: 77-0451; CuO: 80-1916; Nb_2O_5: 80-2493) were used in the analysis of the phases within the samples. The XRD data reveal that only the rutile tin oxide lines are found in pure SnO_2 sample. In the copper oxide doped samples (SCu and SCNb), additional peak (CuO [$\bar{1}$ 1 1]) is evident. However, no niobium oxide peak is found in Nb_2O_5 and CuO-doped tin oxide (SCNb), therefore, it may be due to that Nb ions enter the grains and cannot be detected by XRD. It is similar to that the pentavalent ions are introduced into TiO_2 varistors, where pentavalent ions enter the grains to control the grain conductivity. Further, it is also to be noted that the amount of niobium added in this system is very small, therefore, it is difficult to detect this small amount of niobium by the normal XRD. The phenomenon of the appearance of other phases (copper oxide phases) in the grain boundaries is distinct from the single phase of SnO_2·CoO based ceramic systems previously reported [2–7], which is an interesting thing. This may be explained by the low melting point of copper oxide. CuO will be transformed into Cu_2O at 1122 °C and the melting point of Cu_2O (1236 °C) is lower than that of CoO (1805 °C), it is easy for copper oxide to form liquid when sintering at 1400 °C. As in the CuO doped SnO_2 ceramics, liquid phases sintering mechanism is predominant. In the case of CoO doped SnO_2 ceramics, the oxygen vacancies diffusion mechanism controls the sintering of tin oxide ceramics. Furthermore, by XRD and SEM, we did not obtain other phases in CuO and Ta_2O_5-doped SnO_2 based varistors in another work [8], which may be due to the lower sintering temperature than that of this work. Therefore, the copper oxide into tin oxide, sintered at 1400 °C, is up to saturation, and excess copper oxide that could not enter into tin oxide lattice would centralize at the grain boundaries and prevent the mass transport [9], which was also investigated and confirmed by Nisiro *et al*. [1].

* Author to whom all correspondence should be addressed.

0022-2461
DOI: 10.1007/s10853-005-4231-6

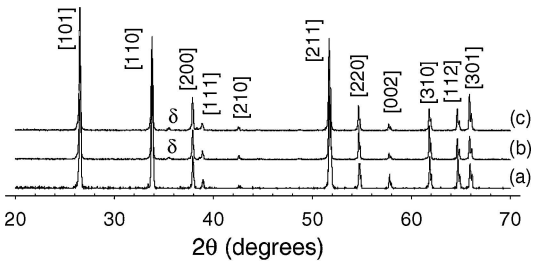

Figure 1 X-ray diffraction patterns of: (a) pure SnO_2, (b) SnO_2·CuO and (c) SnO_2·CuO·Nb_2O_5 ceramic system. δ: CuO [$\bar{1}11$].

The sintered density value, compared to other ceramic systems, is obtained by the Archimedes method and related to the theoretical density of SnO_2 (=6.95 g cm^{-3}), as listed in Table I. The density of tin oxide sintered at above-mentioned condition is 5.55 g cm^{-3}, 80% of the theoretical due to the high vapor pressure of this oxide during sintering. However, when SnO_2 is doped with the copper oxide additives, the densification can be significantly improved at this temperature. In this experiment, we added 1.00 mol% CuO to tin oxide, the density could be up to 6.72 g cm^{-3}, higher than 96% of the theoretical density. As shown in Table I, the density of CuO-doped ceramic system is higher than that of pure SnO_2. In a previous paper [8], the high densification of tin oxide ceramics was attributed to the copper effect in the SnO_2 lattice, which leads to the existence of a liquid phase in the Sn–Cu–O_2 system. This was also studied and confirmed by Dolet and his collaborators [10].

Fig. 2 presents the SEM photomicrographs of SCNb varistor sample compared with the SCTa sample. It is clearly shown the SnO_2 grains are tightly close together with minor copper oxide at grain boundaries. As shown in Table I, the grain size of CuO-doped ceramic system (SC, SCNb and SCTa ceramics) is highly bigger than that of pure SnO_2. Therefore, the introduction of copper oxide not only makes the tin oxide densify, but also advances the grain growth. As donors, the introduction of Nb_2O_5 in small amounts into the SnO_2 ceramics leads to an increase of electronic conductivity in the SnO_2 grains due to substitution of Sn^{4+} for Nb^{5+}, according to the following equation:

$$Nb_2O_5 \xrightarrow{SnO_2} 2Nb_{Sn}^{\cdot} + 2e' + xO_o^x + \frac{5-x}{2}O_2, \quad x = 0-5 \qquad (1)$$

where the Kröger–Vink marks were used. Therefore, by creating the donor, Nb_2O_5 contributes to an increase in the electronic conductivity in the grain, which is similar to the tantalum is introduced into the SnO_2-based varistors [6].

Fig. 3 shows the logarithmic plots of the current density against the applied electrical field for the SCNb varistor system compared with SCTa varistor system. The best nonlinear coefficient ($\alpha = 34.4$) was obtained when doped with the 0.05 mol% concentration of Nb_2O_5. The nonlinear coefficient (α) was obtained by the following equation:

$$\alpha = \frac{\log J_2 - \log J_1}{\log E_2 - \log E_1} \qquad (2)$$

where J_1=10 A m^{-2}, J_2=100 A m^{-2} and E_1 and E_2 are the electrical fields corresponding to J_1 and J_2, respectively. The breakdown electrical field (E_B) was measured at a current density of 10 A m^{-2} and the leakage current density (J_L) was measured at 0.75 E_B. As the important parameters, these varistor parameters are listed in Table II.

The nonlinear electrical parameters could not be obtained for SC system using the above experimental instrument and it shows ohmic electrical behavior with a very high resistivity and has no signs of nonlinearity, as discussed in a previous work [9]. The introduction of

TABLE I Densities and average grain size for samples sintered at 1400 °C for 1 hr

System	ρ (g cm^{-3})	ρ_{rt}^{*} (%)	d (μm)	Reference
SnO_2	5.55	79.9	11.5	This work and [9]
SC	6.72	96.7	17.4	This work and [9]
SCNb	6.56	94.4	18.2	This work
SCTa	6.55	94.2	16.5	This work and [9]

*The theoretical density of SnO_2 is 6.95 g cm^{-3}.

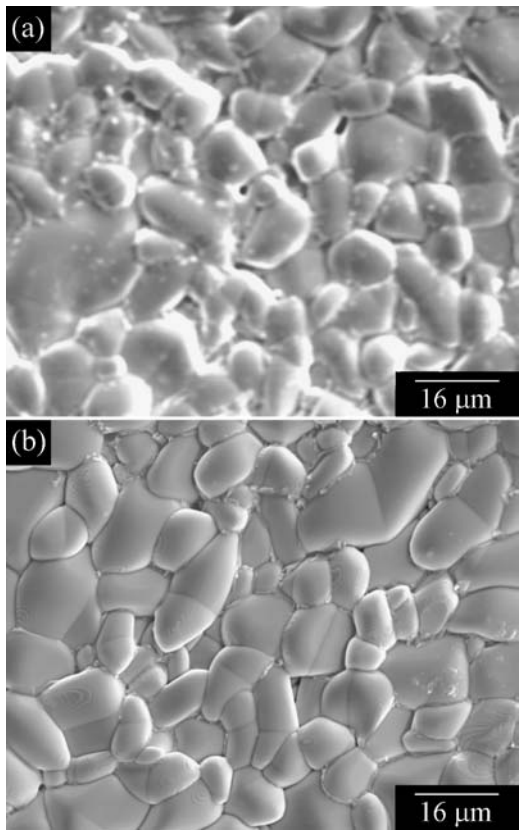

Figure 2 Scanning electron micrographs of the: (a) SnO_2·CuO·Nb_2O_5 and (b) SnO_2·CuO·Ta_2O_5 varistor system.

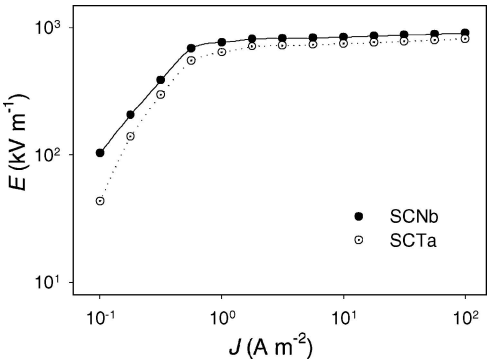

Figure 3 *J–E* characteristics of the SCNb and SCTa varistor system.

either Nb_2O_5 or Ta_2O_5 to the SnO_2·CuO system increases grain conductive, making possible the measurement of the breakdown electrical field of these systems. As shown in Table II, the nonlinear electrical properties are enhanced by the Nb_2O_5 doping as compared with the addition of Ta_2O_5. Further, the leakage current density of SCNb varistor sample is greatly lower than that of SCTa sample. The leakage current originates at the grain boundaries and determines the amount of watt loss that a varistor is expected to generate upon application of a steady-state operating voltage. Therefore, it is an important factor to be considered in varistor fabrication. The SCNb varistor sample has the high nonlinear coefficient ($\alpha = 34.4$) and low leakage current density ($J_L = 2.4\ \mu A\ cm^{-2}$). Therefore, SnO_2·CuO·Nb_2O_5 system is a very beckoning varistor ceramic material and worth to further investigation.

By SEM and XRD, the CuO and Nb_2O_5-doped tin oxide varistors are found to be SnO_2 grains as predominant and minor copper oxide at grain boundaries, while niobium improves the conductive of the grains. The copper oxide intergranular insulating layer separates two semiconductive tin oxide grains and forms the barriers. The electric transport occurs by tunneling across the barriers and is responsible for the electrical nonlinearity of the varistors. Further, the oxygen will be partly adsorbed at SnO_2 grain boundaries and the adsorbed oxygen species may easily capture electrons or react with partial negatively charged defects to become negatively charged ions [6]:

$$O_2 \rightarrow 2O^x_{ad} \quad (3)$$

$$O^x_{ad} + e' \rightarrow O'_{ad} \quad (4)$$

These negatively charged adsorbed oxygen species are essential to the Schottky barrier formation and also responsible for the electrical nonlinearity of the varistors. The role of the adsorbed oxygen in the formation of boundary barriers was studied and confirmed by the literatures [11, 12].

TABLE II Electrical parameters of the SnO_2·CuO·Nb_2O_5 (SCNb) varistor system compared to the SnO_2·CuO·Ta_2O_5 (SCTa) system

System	α	E_B (kV m^{-1})	J_L (μA cm^{-2})	Reference
SCNb	34.4	844	2.4	This work
SCTa	27.3	750	16.4	This work and [9]

In conclusion, the densification of tin oxide could greatly be improved when doped with 1.00 mol% CuO. Furthermore, the introduction of 0.05 mol% Nb_2O_5 into SnO_2·CuO ceramic system would make it possess excellent nonlinearity. The SnO_2·CuO·Nb_2O_5 varistor system was investigated compared to the SnO_2·CuO·Ta_2O_5 system, and the high nonlinearity coefficient $\alpha = 34.4$ and low leakage current density $J_L = 2.4\ \mu A\ cm^{-2}$ was obtained. A modified defect barrier model has been introduced to explain the formation of the grain-boundary barrier. The nonlinear behaviour of SnO_2·CuO·Nb_2O_5 varistor system can be explained by the barrier model. The varistor system of SnO_2·CuO·Nb_2O_5 would be worth of further investigation.

Acknowledgment

Supported by the National Natural Science Foundation of China under the Grant No. 50572056 and the Natural Science Foundation of Shandong Province of China under the Grant No. Z2003F04.

References

1. D. NISIRO, G. FABBRI, G. C. CELOTTI and A. BELLOSI, *J. Mater. Sci.* **38** (2003) 2727.
2. S. A. PIANARO, P. R. BUENO, E. LONGO and J. A. VARELA, *J. Mater. Sci. Lett.* **14** (1995) 692.
3. P. R. BUENO, S. A. PIANARO, E. C. PEREIRA, L. O. S. BULHOES, E. LONGO and J. A. VARELA, *J. Appl. Phys.* **84** (1998) 3700.
4. P. R. BUENO, M. R. DE CASSIA-SANTOS, E. R. LEITE, E. LONGO, J. BISQUERT, G. GARCIA-BELMONTE and F. FABREGAT-SANTIAGO, *ibid.* **88** (2000) 6545.
5. P. R. BUENO, E. R. BEITE, M. M. OLIVEIRA, M. O. ORLANDI and E. LONGO, *Appl. Phys. Lett.* **79** (2001) 48.
6. C. M. WANG, J. F. WANG, H. C. CHEN, W. X. WANG, W. B. SU, G. Z. ZANG and P. QI, *J. Phys. D: Appl. Phys.* **36** (2003) 3069.
7. S. R. DHAGE and V. RAVI, *Appl. Phys. Lett.* **83** (2003) 4539.
8. C. M. WANG, J. F. WANG, W. B. SU, G. Z. ZANG and P. QI, *Mater. Lett.* **59** (2005) 201.
9. *Idem.*, *J. Mater. Sci.* **40**(24) (2005).
10. N. DOLET, J. M. HEINTZ, L. RABARDEL, M. ONILLON, and J. P. BONNET, *ibid.* **30** (1995) 365.
11. F. STUCKI, F. GREUTER, *Appl. Phys. Lett.* **57** (1990) 446.
12. P.R. BUENO, E.R. BEITE, M. M. OLIVEIRA, M. O. ORLANDI and E. LONGO, *ibid.* **79** (2001) 48.

Received 18 May
and accepted 12 July 2005